



**HAL**  
open science

## Can small reservoirs be used to gauge stream runoff?

Jérôme Molenat, Cécile Dagès, Maroua Bouteffeha, Insaf Mekki

### ► To cite this version:

Jérôme Molenat, Cécile Dagès, Maroua Bouteffeha, Insaf Mekki. Can small reservoirs be used to gauge stream runoff?. *Journal of Hydrology*, 2021, 603, pp.127087. 10.1016/j.jhydrol.2021.127087. hal-03478167

**HAL Id: hal-03478167**

**<https://hal.inrae.fr/hal-03478167>**

Submitted on 8 Jun 2022

**HAL** is a multi-disciplinary open access archive for the deposit and dissemination of scientific research documents, whether they are published or not. The documents may come from teaching and research institutions in France or abroad, or from public or private research centers.

L'archive ouverte pluridisciplinaire **HAL**, est destinée au dépôt et à la diffusion de documents scientifiques de niveau recherche, publiés ou non, émanant des établissements d'enseignement et de recherche français ou étrangers, des laboratoires publics ou privés.



Distributed under a Creative Commons Attribution - ShareAlike 4.0 International License

# 1 Can small reservoirs be used to gauge stream runoff?

2 Jérôme Molénat<sup>(1,\*)</sup>, Cécile Dagès<sup>(1)</sup>, Maroua Bouteffeha<sup>(2)</sup>, Insaf Mekki<sup>(3)</sup>

3 (1) LISAH, Univ. Montpellier, INRAE, IRD, Institut Agro, Montpellier, France

4 (2) Laboratory of Modelling in Hydraulics and Environment, National Engineering School of Tunis (ENIT), University of Tunis El Manar,

5 Box 37, Le Belvédère Tunis 1002, Tunisia

6 (3) INRGREF, Tunis, Tunisia

ACCEPTED VERSION

## 7 **Abstract**

8 Understanding stream runoff generation processes requires distributed stream runoff estimates ; however the acquisition of  
9 such estimates remains challenging in hydrology, especially in remote areas. In regions with a high spatial density of small  
10 reservoirs, those reservoirs could be employed to gauge stream runoff (Liebe *et al.*, 2009). Using a water balance approach,  
11 the stream runoff flowing into a reservoir from a drainage catchment could be estimated. Accordingly, this work aims to  
12 address the following two questions: i) what is the error in the estimated stream runoff and ii) what are the main estimation  
13 uncertainty factors? Based on a case study of the Kamech catchment, Tunisia, stream runoff was estimated at different  
14 temporal resolutions (1-32 days), and a global sensitivity analysis was performed to estimate the contributions of the  
15 reservoir water balance terms (evaporation, rainfall, percolation, reservoir water level and level-area-volume relations) to the  
16 estimated stream runoff uncertainty.

17 The results reveal that stream runoff can be reliably estimated based on small reservoirs using a mass balance approach.  
18 The error and global stream runoff estimation uncertainties decrease as the temporal resolution increases. The bathymetric  
19 relationships (level-area and level-volume relations) constitute a strong factor of uncertainty for all temporal resolutions, and  
20 even the dominant factor for temporal resolutions ranging from 4 to 23 days. The estimation uncertainty for the shortest  
21 temporal resolutions (1-8 days) mainly originates from reservoir level uncertainty. As the temporal resolution increases, the  
22 contribution of percolation uncertainty increases. The general (not site-specific) conclusions of this study are that stream  
23 runoff gauging based on small reservoirs requires the determination of the bathymetric relations and that small reservoirs  
24 could be used as reliable stream runoff gauges at short temporal resolutions if the reservoir level is measured with limited  
25 uncertainty and at long temporal resolutions as long as the percolation rate from the reservoir is known with limited  
26 uncertainty.

27 **keywords**

28 gauging stream runoff, reservoir water balance, uncertainty, global sensitivity analysis,

29 **Highlights**

- 30 • Small reservoirs could be used to gauge catchment stream runoff
- 31 • Stream runoff is estimated based on a small reservoir using the water balance approach
- 32 •
- 33 • High stream runoff are better estimated than low ones
- 34 •
- 34 • The performance of estimation improves as the temporal resolution increases [1d-32d]
- 35 • Bathymetric relations, percolation and reservoir level estimation are the main sources of uncertainty

## 36 **Introduction**

37 Stream runoff time series constitute basic and critical data in hydrology that are needed to better understand the  
38 mechanisms underlying the variability and generation of stream runoff and are essential for quantifying the status of water  
39 resources and planning and implementing management operations. Stream runoff data are important for hydrological  
40 modelling performed for both scientific and operational objectives. These time series are also necessary for understanding  
41 the biogeochemical cycles and ecological functioning of streams. However, acquiring either local (at a point) or spatially  
42 distributed stream runoff time series data remains a real challenge in hydrology; this challenge is particularly acute in remote  
43 areas, such areas in arid and semi-arid environments.

44 Small reservoirs have been erected in arid and semi-arid locales for supplying water (often for agriculture) and preventing  
45 downstream flooding. Despite the lack of a formal definition, a small reservoir is commonly characterised by a storage  
46 capacity smaller than 1 Mm<sup>3</sup> (Habets *et al.*, 2018). A small reservoir often consists of a small dam built across a valley to  
47 intercept and store stream runoff. For decades, small reservoirs have been increasingly constructed in many countries.  
48 Consequently, in some catchments,, such as those in Australia (Schreider *et al.*, 2002 ; Nathan & Lowe, 2002) and in South  
49 Africa (Hughes & Mantel, 2010), the density can exceed 1 reservoir/km<sup>2</sup>. The idea to use small reservoirs as stream gauges  
50 has already been examined (Albergel & Rejeb, 1997 ; Mekki *et al.*, 2006 ; Liebe *et al.*, 2009). Liebe *et al.* (2009) used a  
51 simple hydrological model coupled with the remote monitoring of a small reservoir to simulate daily stream runoff time series  
52 for a catchment in Ghana. Furthermore, using the water balance approach, the water levels in small reservoirs have been  
53 continuously monitored to estimate stream runoff, for instance, in Tunisia by Albergel and Rejeb (1997) and Mekki *et al.*  
54 (2006). The technological development of automatic water level sensors and remote data transmission and the development  
55 of community-based approaches (Starkey *et al.*, 2017), could enhance the availability of data for the evaluation of the water  
56 balance and thus improve the use of small reservoirs as stream runoff gauges.

57 The objective of this study is to examine the relevance of regarding small reservoirs as stream gauges based on the water  
58 balance approach. This study relies on the Kamech catchment, Tunisia, which is a research catchment draining into a small

60 reservoir. We followed a two-step approach. In the first step, the stream runoff was estimated at different temporal  
61 resolutions based on the reservoir water balance; then, the estimated time series data were compared with stream runoff  
62 measurements obtained from a classic stream gauge station. To evaluate the adding value of the reservoir method, we also  
63 estimated, as a comparison, stream runoff based on a more straightforward method used in engineering hydrology which is  
64 the runoff coefficient. In the second step, a global sensitivity analysis was performed to identify and quantify the main  
65 sources of uncertainty in the stream runoff estimated using the reservoir water balance approach. Based on these results,  
66 the feasibility of considering small reservoirs as stream gauges is discussed.

## 67 **1. Study catchment and data**

68 The Kamech catchment is a small catchment (2.63 km<sup>2</sup>) located in northern Tunisia. The Kamech catchment is one of the  
69 two catchments in France and Tunisia of the observatory OMERE (an acronym for Mediterranean Observatory of Rural  
70 Environment and Water or « Observatoire Méditerranéen de l'Environnement Rural et de l'Eau », in French) (Molénat *et al.*,  
71 2018); the catchment also belongs to the French network of critical zone observatories called OZCAR (Gaillardet *et al.*,  
72 2018). The catchment characteristics, equipment and monitoring are extensively described in Molénat *et al.* (2018).  
73 Climatically, the region is semi-arid to sub-humid, and the 25-year mean annual rainfall and reference evaporation are  
74 645mm and 1366mm, respectively.

75 In 1992, a dam was built across the wadi at the catchment outlet to prevent siltation in a large downstream dam. The  
76 reservoir has a capacity of 135,000 m<sup>3</sup> (Figure 1). The reservoir intercepts runoff from the wadi and lateral surface runoff  
77 along its banks. The water within the reservoir may be withdrawn for irrigation in spring and summer, and water can also be  
78 released when the reservoir reaches its capacity to ensure the safety of the dam's infrastructure. In the present study, we  
79 chose the water year 2011-2012 during which releases and withdrawals were either null or negligible.

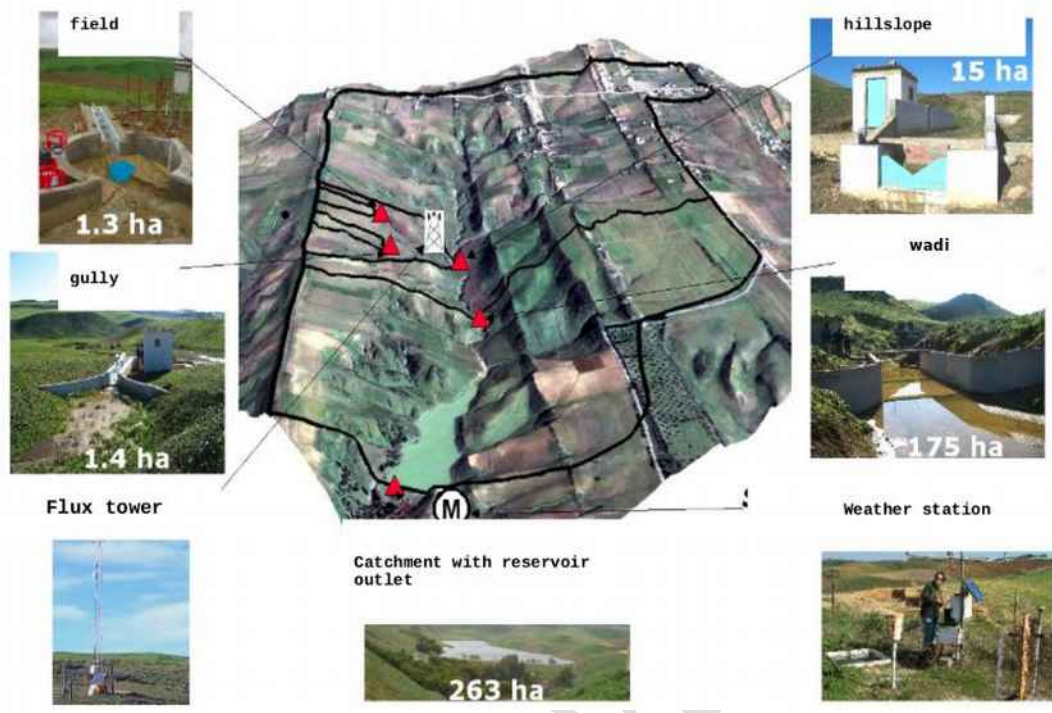
80 Hereafter, we present the available data by estimating the relative or absolute errors in each measurement, as these errors  
81 are particularly important for the global sensitivity analysis performed in this work. Rainfall in the catchment is measured  
82 using a tipping bucket gauge located on the dam. In this work, the hourly mean rainfall rate is used. The relative error in a  
83 rainfall measurement acquired by a tipping bucket depends on many factors, such as the rainfall intensity and volumes of the  
84 compartments within the bucket; consequently, the relative errors vary considerably in the literature (Habib *et al.*, 2001 ;  
85 Wang *et al.*, 2008). In this work, we assumed a relative error of 20% in the rainfall measurements corresponding to the  
86 highest values of an hourly time step reported in previous studies (Wang *et al.*, 2008). Pan evaporation is measured daily  
87 using a pan located on a bank of the reservoir near the dam. The hourly evaporation rate was derived from daily records  
88 considering a sinusoidal hourly variation each day. Evaporation from the reservoir water free surface  $e_{fs}$  in the reservoir was  
89 derived from pan evaporation  $e_{pan}$  considering a pan coefficient,  $k$ , of 0.65 (Bouteffeha *et al.*, 2015) according to  $e_{fs}=k.e_{pan}$ . In  
90 general, the  $k$  factor can vary across reservoirs and within a given reservoir over time. Regarding lake or reservoir  
91 evaporation,  $k$  is generally found to be lower than 1.0 with wide variations ranging from 0.5 to 1.2 (e.g. Fu *et al.*, 2004;  
92 Martinez Alvarez *et al.*, 2007). In this work we considered both the error associated with pan evaporation measurements,  
93  $e_{pan}$ , and the error associated with the determination of the pan coefficient,  $k$ . By applying a logarithmic transform of the latter  
94 relation and then deriving, we can deduce that  $de_{fs}/e_{fs}=dk/k+de_{pan}/e_{pan}$  where  $de_{fs}$ ,  $dk$  and  $de_{pan}$  are the derivatives of  $e_{fs}$ ,  $k$  and  
95  $e_{pan}$ , respectively, that are assimilated in the absolute error. Thus, the relative error in  $e_{fs}$ ,  $de_{fs}/e_{fs}$ , is the sum of the relative  
96 errors in  $e_{pan}$  and  $k$ . Following Winter (1981), the relative errors in the pan evaporation and pan coefficient estimation were  
97 considered to be 20% and 10%, respectively, yielding to a relative error of 30% in the reservoir water evaporation estimation.  
98 The reservoir water level is measured every 5 minutes by a continuous pressure probe compensating for atmospheric  
99 pressure fluctuations. The absolute error in the water level measurement was estimated at 20 mm independent of the level.  
100 This error includes the error due to the sensor considered as independent of the level according to the manufacturer and the  
101 error resulting from wind-induced variations which was considered empirically at approximately 15 mm and independent of  
102 the level. The reservoir water volume can be derived from the relations between the water volume and level and between the  
103 water area and level, hereafter named the level-volume (L-V) and level-area (L-A) relations, respectively. These relations  
104 were determined based on a bathymetric survey performed in August 2008. The bathymetric survey produced bipoints of L-

105  $V_i$  and  $L_i-A_i$ . The relations L-V and A-V were fitted on the bi-points as  $V=aL^b$  and  $A=cL^d$ . Error in the relations are derived  
106 from different sources as follows: data source error derived from the topographic survey of the reservoir bed elevation (error  
107 in measurement, sampling interval and DEM building) and error in the volume and area calculations. For each bi-point, *i.e.*,  
108  $L_i-V_i$ , or  $L_i-A_i$ , we considered that the volume  $V_i$ , or area  $A_i$ , was estimated with a relative error of 20%.

109 The percolation from the reservoir was estimated according to Bouteffeha *et al.* (2015), who estimated the percolation rates  
110 at some reservoir water levels. A linear regression was performed, allowing us to estimate the percolation rate at each  
111 reservoir water level. Thus, the relation between the percolation rate and water level, hereafter named the percolation  
112 relation, was based on different data than those used in the present study to estimate stream runoff. The error in the  
113 percolation estimation was fixed from the 99% confidence interval. In a linear regression, the confidence interval depends on  
114 the value of the regressor and is not theoretically constant; in our case, the errors in the percolation rates within the range of  
115 reservoir water levels varied between 2.18 and 2.19 mm/day. Consequently, the error in the percolation rate estimation was  
116 assumed to be constant at 2.185 mm/day.

117 In the Kamech catchment, the wadi runoff is monitored with a gauging station located upstream of the reservoir mouth (wadi  
118 station in Figure 1). The station is located sufficiently upstream of the reservoir mouth to avoid or minimize backwater effects  
119 (Figure 1). The station is equipped with a U-shaped concrete flume. The water level in the flume is measured once per  
120 minute by a pressure transducer sensor and recorded in a data logger. Then, a stage-discharge relationship is used to  
121 estimate stream runoff based on the water level. A set of ten stage-discharge values was used to establish the stage-  
122 discharge relationship. For every stage-discharge value, the discharge was estimated by the velocity-area method. Velocity  
123 in the wet section was measured with a velocimeter every 2 cm of depth and at lateral intervals proportional to water level.  
124 Hourly runoff averages were used in this work, and the total runoff entering the reservoir was calculated as the area-scaled  
125 specific runoff measured in the wadi.

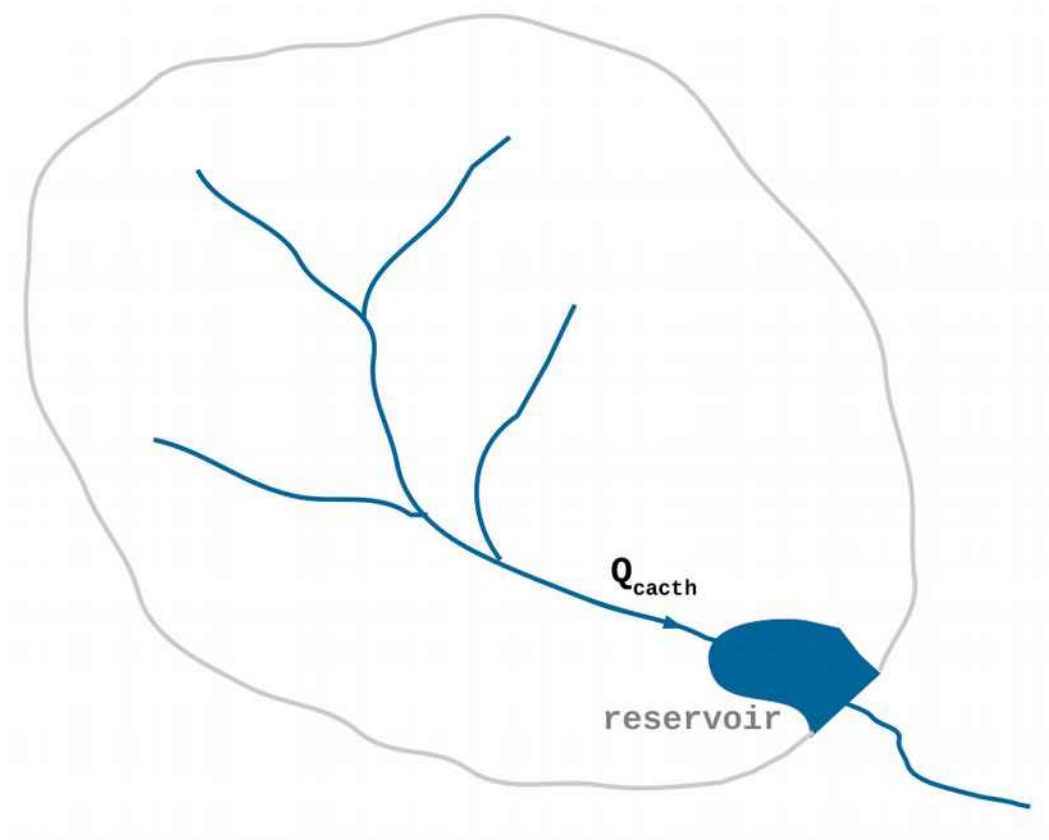




126 Figure 1 : Aerial view of the Kamech catchment showing the reservoir and locations of the weather station and wadi gauge  
 127 station.

128 **2. Estimated stream runoff and associated error and uncertainty**

129 **2.1. Estimation of stream runoff**



130 *Figure 2 : Schematic view of a catchment draining into a small reservoir.  $Q_{catch}$  represents the catchment stream runoff*  
131 *flowing into the reservoir.*

132 The small reservoir considered here captures the stream runoff draining from an upstream catchment (Figure 2). Hence, the  
133 temporal variations in the reservoir water volume depend on the upstream stream runoff and other inflows (rainfall directly

134 impacting the surface water) and outflows (evaporation from the surface water and seepage through the reservoir bed and  
 135 dam). Here, water abstraction is assumed to be null or negligible. The variation in the reservoir water volume at a temporal  
 136 resolution of  $\Delta t$  [T] can be expressed based on the water balance as follows:

$$137 \quad \frac{\Delta V}{\Delta t} = q \cdot A_c - E + R - S_p \quad \text{Equation (1)}$$

138 where  $\Delta V$  is the variation in the reservoir water volume  $L^3$  over the given time step  $\Delta t$ ,  $q$  is the catchment-specific runoff [L/T]  
 139 flowing into the reservoir over the given time step,  $E$  is the evaporation flux [ $L^3/T$ ] from the reservoir surface water over the  
 140 given time step,  $R$  is the mean rainfall flux [ $L^3/T$ ] at the reservoir surface water over the given time step,  $S_p$  is the mean  
 141 percolation flux [ $L^3/T$ ] from the reservoir water surface as infiltration occurs through the reservoir bottom or wall dams, and  $A_c$   
 142 is the catchment area [ $L^2$ ] drained by the reservoir. From Equation (1), the specific stream runoff over a given time step  $\Delta t_i$  is  
 143 estimated as:

$$144 \quad q_i^{est} = \frac{1}{A_c} \left( \frac{(V_i^{fin} - V_i^{ini})}{\Delta t_i} - R_i + E_i + S_{p_i} \right) \quad \text{Equation (2)}$$

145 where  $V_i^{fin}$  [ $L^3$ ] and  $V_i^{ini}$  [ $L^3$ ] are the final and initial water volumes in the reservoir, respectively, at the end and the beginning of  
 146 the given time step and  $q_i^{est}$ ,  $E_i$ ,  $R_i$  and  $S_{p_i}$  are the estimated specific stream runoff [L/T], rainfall flux [ $L^3/T$ ], evaporation flux  
 147 [ $L^3/T$ ] and percolation flux [ $L^3/T$ ], respectively, over the given time step  $\Delta t_i$ . The percolation was calculated based on a linear  
 148 regression of the reservoir water level and percolation rate. At each time step of a given temporal resolution, the evaporation,  
 149 rainfall and percolation fluxes were estimated as the product of the water surface area of the reservoir and the cumulative  
 150 evaporation, rainfall and percolation, respectively, over the time step. The surface area and volume of water in the reservoir  
 151 were calculated based on the water level measurements and the L-A and L-V relations, respectively. The average surface  
 152 area over a given time step was considered to be the mean of the initial and final surface areas of the time step.

153 The specific stream runoff in one hydrologic year ranging from 01 September 2010 to 31 August 2011 was calculated. The  
154 stream runoff times series were calculated for 32 temporal resolutions  $\Delta t$  ranging from 1 day to 32 days with a one-day  
155 increment. The length of the stream runoff time series ranged from 365 steps at the 1-day resolution to 11 steps at the 32-  
156 days resolution.

157 The interest of using the small reservoir method to estimate stream runoff was analysed based both on performance criteria of estimation  
158 (see the following section) and on a comparison with a simple method. The runoff coefficient method was used as the simple method,  
159 since it is particularly relevant to Hortonian runoff catchments, such as Kamech catchment (Hingray et al., 2014). According to this  
160 method, the stream runoff is estimated at a constant fraction of the rainfall. We explored the values of runoff coefficient ranging from 0.01  
161 to 0.5. For every value and at every time resolution (1 to 32 days), the Nash-and-Sutcliffe efficiency was calculated from the observed  
162 and estimated stream runoff. We retained the value of 0.09 as runoff coefficient, which provided the highest efficiency mean calculated  
163 from the efficiencies of all the time resolutions.

## 164 **2.2. Estimation error, uncertainty and performance**

165 The following two types of uncertainty sources were considered in the analysis of uncertainty in the stream runoff estimation  
166 based on Equation (2): the measurement uncertainty and the derived data uncertainty (McMillan et al., 2018). The  
167 measurement uncertainty was associated with errors in the direct and local measurements of the pan evaporation, rainfall  
168 rate by rain gauging and reservoir water level by a pressure sensor. The derived data uncertainty in the reservoir water  
169 volume and area, the evaporation flux and the percolation flux was considered. The derived data uncertainty in the water  
170 volume and area ( $V_i$  and  $A_i$  in Equation 2) was assumed to result from the uncertainty in the L-V and L-A relations. The  
171 uncertainty in the percolation rate ( $Sp_i$  in Equation 2) was assumed to mainly originate from the uncertainty in the percolation  
172 relation. At least, the derived data uncertainty associated with the evaporation flux ( $E_i$  in Equation 2) was assumed to  
173 originate from the uncertainty in the pan coefficient. Each uncertainty was assumed to vary from time step to time step when  
174 applying Equation 2.

175 As a consequence of the measurement uncertainty and the derived data uncertainty, each variable in Equation (2) was  
176 considered a random variable characterised by a probability density function (pdf). The range of values defined by the pdf of  
177 a given term corresponds to the range of possible values due to the errors potentially occurring in the estimation of that term

178 The stream runoff at each  $\Delta t_i$  was also considered a random variable with possible values. Therefore, for each time step  $\Delta t_i$   
179 during a given simulation period (e.g., a water year), we defined the following:  $q_i^{est}$ , a possible value of the stream runoff  
180 during  $\Delta t_i$ ;  $\overline{q_i^{est}}$ , the estimated stream runoff during  $\Delta t_i$  as the mean of all possible values; and  $U_{q_i}$ , the uncertainty in the  
181 estimated stream runoff at  $\Delta t_i$ , where the true value  $q_i$  is in the interval  $[\overline{q_i^{est}} - U_{q_i}; \overline{q_i^{est}} + U_{q_i}]$  with a certain level of  
182 confidence. With the 99% level of confidence we chose, the uncertainty is equal to  $3.0 \sigma_{q_i}/\sqrt{n}$ , where  $\sigma_{q_i}$  is the standard  
183 deviation of  $n$  possible values.

184 The error in the estimation,  $\varepsilon_{q_i}$ , was considered the difference between the mean estimated stream runoff,  $\overline{q_i^{est}}$ , and the  
185 unknown true stream runoff,  $q_i^{catch}$ . Then, the mean error (ME) and the mean uncertainty (MU) of the catchment stream runoff  
186 over the given simulation period are the averages of the errors,  $\varepsilon_{q_i}$ , and uncertainties,  $U_{q_i}$ , respectively, where  $i$  ranges from 1  
187 to  $n$  with  $n$  being the total time step considered during the given period. The Nash-Sutcliffe efficiency was calculated as the  
188 estimation performance criterion considering the stream runoff ( $NSE$ ) and the square root of the stream runoff ( $NSE_{sqrt}$ ). The  
189 motivation to consider the square root transform is to reduce the weights of the high stream runoff values in the analysis of  
190 the stream runoff estimates.

### 191 2.3. Global sensitivity analysis

192 A global sensitivity analysis (GSA) was performed based on Sobol's method, which is a variance-based method (Sobol *et al.*,  
193 2001). The output of a model with a discrete time step can be expressed as follows:

$$194 \quad y = f(x, \theta) \quad \text{Equation (3)}$$

195 where  $y$  is the output variable of the model,  $x$  is the input variable and  $\theta$  is the parameter set. The variables  $y$  and  $x$  and the  
196 parameter  $\theta$  can be scalar or vectors. Sobol's method evaluates the variance of  $y$  caused by changes in the input,  $x$ , and the

197 parameter set  $\theta$ . Therefore, both the input variables and the parameters can be factors in the sensitivity analysis. Typically,  
 198 the direct model output,  $y$ , is replaced by a model performance measure of the stream runoff prediction (Tang *et al.*, 2007).  
 199 Thus, a sensitivity analysis applies a measure of the error between the observed and simulated values. In the present work,  
 200 the root mean square error (RMSE) between the observed and estimated stream runoff was chosen as the performance  
 201 measure. Considering  $y$  a random variable described by a pdf  $Y$ , the total variance of  $y$  can be decomposed as follows:

$$202 \quad \text{Var}(y) = \sum_i^p \text{Var}_i + \sum_{i < j = 1}^p \text{Var}_{ij} + \sum_{i < j < k = 1}^p \text{Var}_{ijk} + \dots + \text{Var}_{1,2,\dots,p} \quad \text{Equation (4)}$$

203 where  $\text{Var}(y)$  is the total variance of the output variable,  $y$ , due to  $p$  factors,  $p$  is the number of factors, and  $\text{Var}_i$  is the  
 204 variance attributable to the principal effect of factor  $i$ , while the factors are the input variables  $x$  and/or parameters  $\theta$ , and the  
 205 other terms corresponding to the fraction of the total variance attributable to the interaction effects between the factors. The  
 206 interaction reflects how the factors intensify, cancel, or compensate for the effects of the other factors in the model outputs  
 207 (Razavi and Gupta, 2015). Based on the variance decomposition of  $y$ , the following two indices are defined:

$$208 \quad S_i = \frac{\text{Var}_i}{\text{Var}(y)} \quad \text{Equation (5)}$$

209 and

$$210 \quad S_{Ti} = 1 - \frac{\text{Var}_{-i}}{\text{Var}(y)} \quad \text{Equation (6)}$$

211 where  $S_i$  and  $S_{Ti}$  are the first-order Sobol index and total Sobol index, respectively, and  $\text{Var}_{-i}$  is the variance attributable to all  
 212 factors except for  $i$ .

213 The GSA aims to study the sensitivity of the model simulation to various factors. In contrast to the usual GSA, where the  
 214 model parameters are the factors (e.g., Tang *et al.*, 2007), in our study, the factors are the variables used in Equation (2) to

215 simulate stream runoff. Actually, each variable used in Equation (2) corresponds to a vector, i.e., a time series. Therefore,  
216 the Sobol indices were calculated from a large number of simulations of stream runoff time series, and each simulation was  
217 performed with a sampled time series of each variable in Equation (2). In practice, considering a given temporal resolution  
218  $\Delta t$ , a large number of sampled time series of the initial water level at the beginning of each time step, the final water level at  
219 the end of each time step, the rain, the evaporation and the percolation were generated. Furthermore, for each simulated  
220 time series of stream runoff, we considered a possible L-A relation and a possible L-V relation (see the following section).  
221 Ultimately, the following six factors were considered in the GSA : i) initial water level ii) final water level, iii) rain, iv)  
222 evaporation, v) percolation and vi) bathymetric relations (L-A and L-V relations).

## 223 **2.4 Implementation of estimations**

224 For each temporal resolution  $\Delta t$ , we estimated  $n=10,000$  possible time series of stream runoff. As a result, we obtained  $n$   
225 estimations of the stream runoff,  $q^{\text{est}}$ , for each given time step  $\Delta t$ . Each possible time series of runoff was obtained with all  
226 possible time series of all terms on the right side of Equation (2). To generate a possible time series for each term on the  
227 right side, we proceeded as follows. For each variable or derived variable used in Equation (2) and associated with  
228 uncertainty, a possible value at each time step was drawn from a pdf. We assigned a pdf to each variable associated with  
229 measurement uncertainty and derived data uncertainty. A given pdf characterised by a mean and a standard deviation was  
230 considered at each time step for each term. Following previous studies (Horner *et al.*, 2018), the error associated with water  
231 level measurement was assumed to follow a Gaussian distribution. The mean was considered the measured value and the  
232 standard deviation was fixed at the absolute error in the measurement. The percolation rate was also assumed to follow a  
233 Gaussian distribution with a mean equal to the value derived from the percolation relation and a standard deviation  
234 corresponding to the prediction error at the 99 % confidence interval in the linear regression used as the percolation relation.  
235 Regarding the other terms (rainfall and evaporation), due to lack of real distribution or tangible evidence of the shape of the  
236 pdf, we chose a uniform distribution. This choice, leads to maximizing the uncertainty compared to that of other distributions.  
237 At each time step, the mean was considered the measured value, and the standard deviation was derived from the relative

238 error associated with the rainfall measurement and evaporation estimation. The relative errors were fixed at 20% for rainfall  
239 and 30% for the evaporation rate (see section 1).

240

241 To estimate  $n$  possible time series of stream runoff,  $n$  possible L-V and L-A relations were also established randomly by  
242 considering the uncertainty in these relations. To establish each possible relation, we considered that each  $V_i$  and  $A_i$   
243 measurement used to fit the L-V and L-A relations is characterised by a specific uniform pdf with a mean corresponding to  
244 the measured value and a standard deviation derived from the standard error in the measurement (section 1). To estimate  
245 each possible time series of stream runoff, we first randomly drew each  $V_i$  and  $A_i$  and then fitted the possible L-V and L-A  
246 relation to the generated  $L_i$ - $V_i$  and  $L_i$ - $A_i$  bipoins.

247 Then, the estimated stream runoff at a given time step was calculated as the mean of all 10,000 simulated possible values.  
248 The uncertainty in the estimated stream runoff was calculated based on the standard deviation of the 10,000 simulated  
249 possible values. Then, the error in the simulated stream runoff at a given time step corresponded to the absolute difference  
250 between the observed value and the simulated mean value. In each temporal resolution, the mean error and mean  
251 uncertainty were calculated, corresponding to the means of the errors and uncertainties, respectively, of each simulated  
252 stream runoff in the time series. The Nash-Sutcliffe efficiency metrics (NSE and  $NSE_{\text{sqrt}}$ ) were also calculated based on the  
253 observed values and simulated mean values.

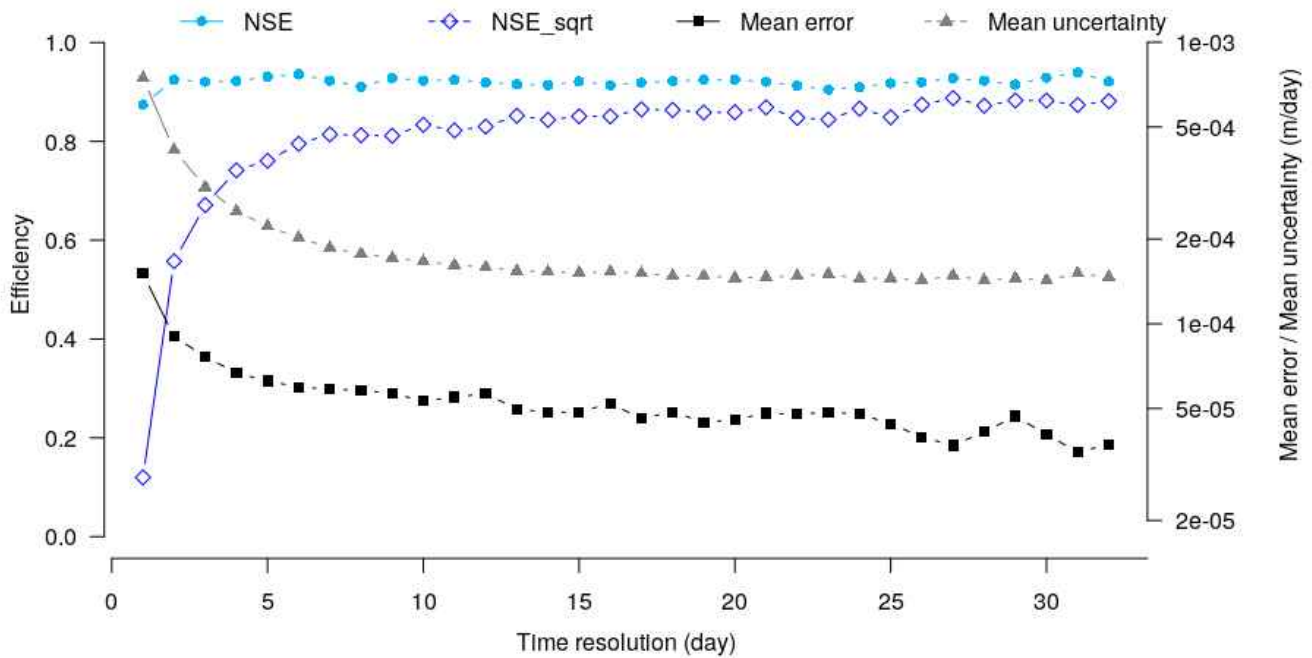
## 254 **3. Results**

### 255 **3.1 Error and total uncertainty**

256 Considering the simulation performance, stream runoff is fairly well estimated based on the water balance approach



257 regardless of the temporal resolution considered (Figure 3). The Nash-Sutcliffe criteria are greater than 0.87 at all temporal  
 258 resolutions and greater than 0.91 at  $\Delta t \geq 27$  days. The RMSE decreases as the temporal resolution increases up to 6 days,  
 259 and then the RMSE slightly decreases. The largest RMSE (at a temporal resolution of 1 day) is  $1.88 \times 10^{-4}$  m/day, while the  
 260 smallest RMSE is  $5.8 \times 10^{-5}$  m/day at a temporal resolution of 32 days.

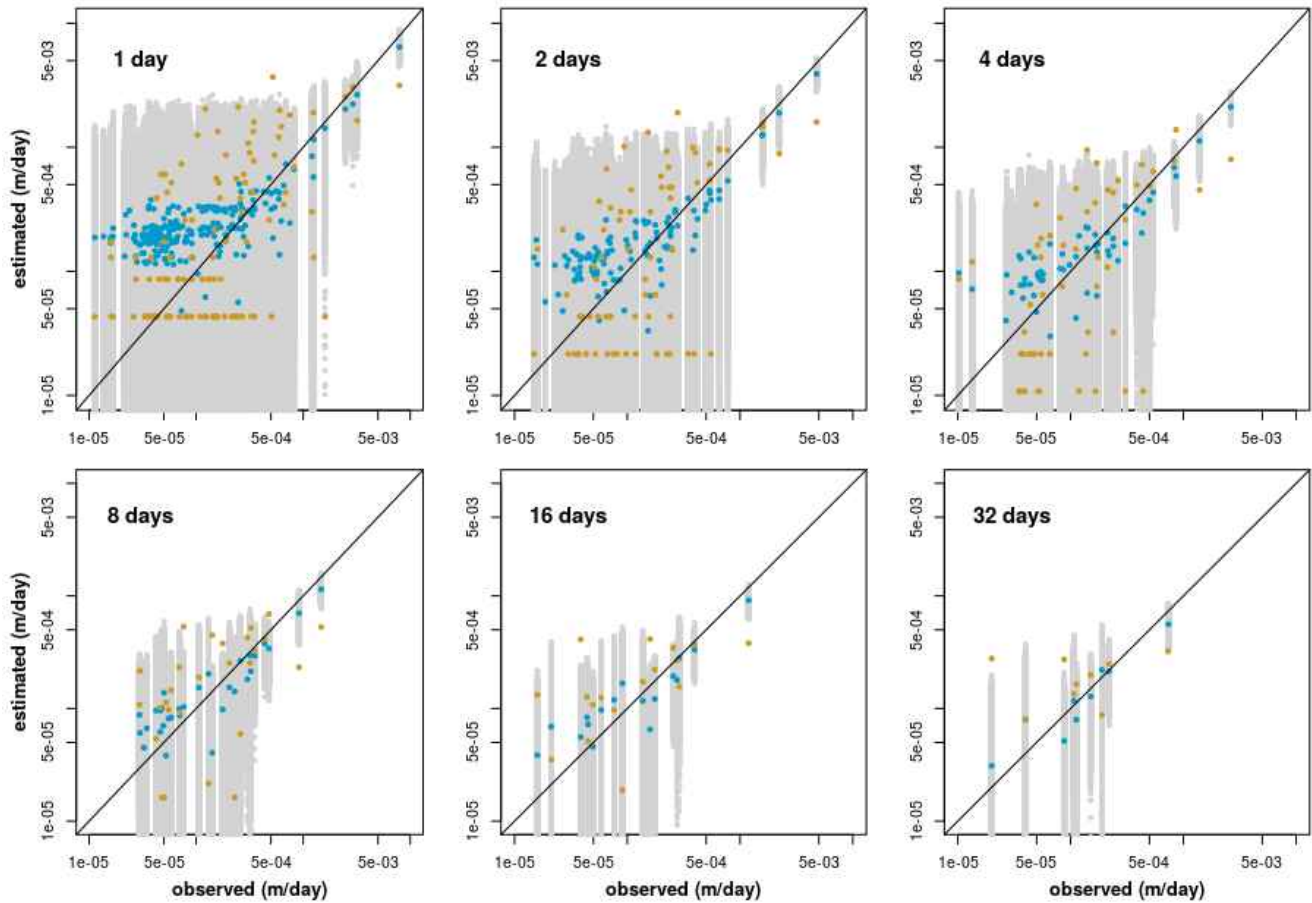


261 Figure 3 : Nash efficiencies calculated based on the stream runoff values NSE (blue points) and the square roots of the  
 262 values  $NSE_{sqrt}$  (blue diamonds) on the left y-axis and the RMSE (black squares) and mean uncertainty in the stream runoff  
 263 estimation (grey triangles) on the right y-axis at temporal resolutions ranging from 1 day to 32 days.

264 The  $NSE_{sqrt}$  criteria are more variable than the common NSE depending on the temporal resolution.  $NSE_{sqrt}$  increases from  
 265 0.12 to 0.88 as the resolution increases from 1 day to 32 days, implying that low stream runoff is globally simulated the worst  
 266 at the finest temporal resolution. A comparison of the simulated and observed stream runoff values at varying temporal

267 resolutions (Figure 4) confirms these results. A large discrepancy is observed in the lowest stream runoff values (smaller  
268 than  $5.0 \times 10^{-4}$  m/day) at fine temporal resolutions (1 day and 2 days). Regarding larger temporal resolutions (greater than 8  
269 days), the discrepancy in the same range of stream runoff values is much smaller.

270 The mean uncertainty exhibits a strong decreasing trend at temporal resolutions between 1 day and 8 days but remains  
271 relatively constant at resolutions longer than 8 days. The relative mean uncertainty was calculated for each estimated stream  
272 runoff as the quotient of the mean of the estimated values over the standard deviation of the estimated values ; then, we  
273 derived the mean relative uncertainty corresponding to the mean of all relative uncertainty values during the simulation  
274 period. The mean relative uncertainty decreases from 1.16 to 0.51 as the temporal resolution increases from 1 day to 32  
275 days. Furthermore, the relative uncertainty of low stream runoff seems to be greater than for that of the highest stream runoff  
276 as illustrated by the spread of the grey squares in Figure 4. To quantify the visual interpretation of Figure 4, the mean relative  
277 uncertainty was also calculated considering the following two classes of stream runoff values: one class corresponding to  
278 stream runoff values smaller than the threshold of  $5 \times 10^{-4}$  m/day, *i.e.*, low stream runoff, and one class corresponding to  
279 stream runoff values larger than this threshold, *i.e.*, values considered representative of medium to high stream runoff. At all  
280 temporal resolutions, the mean relative uncertainty of the low stream runoff class is much greater than that for the  
281 medium/high stream runoff class. In both classes, the mean relative uncertainty decreases as the temporal resolution  
282 increases. The mean relative uncertainty of the low stream runoff class is 1.21 (121%) and 0.55 (55%) at temporal  
283 resolutions of 1 day and 32 days, respectively. Regarding the high stream runoff values, the mean relative uncertainty is 0.67  
284 (67%) and 0.12 (12%) for temporal resolutions of 1 day and 32 days, respectively.



285 Figure 4 : Estimated versus observed stream runoff [m/day] at six time steps ranging from 1 to 32 days. The estimated value  
 286 by the reservoir method correspond to the blue points. The estimated values with the runoff coefficient method correspond to  
 287 the golden points. Each light grey point corresponds to one estimation. The 1:1 line is indicated in black.

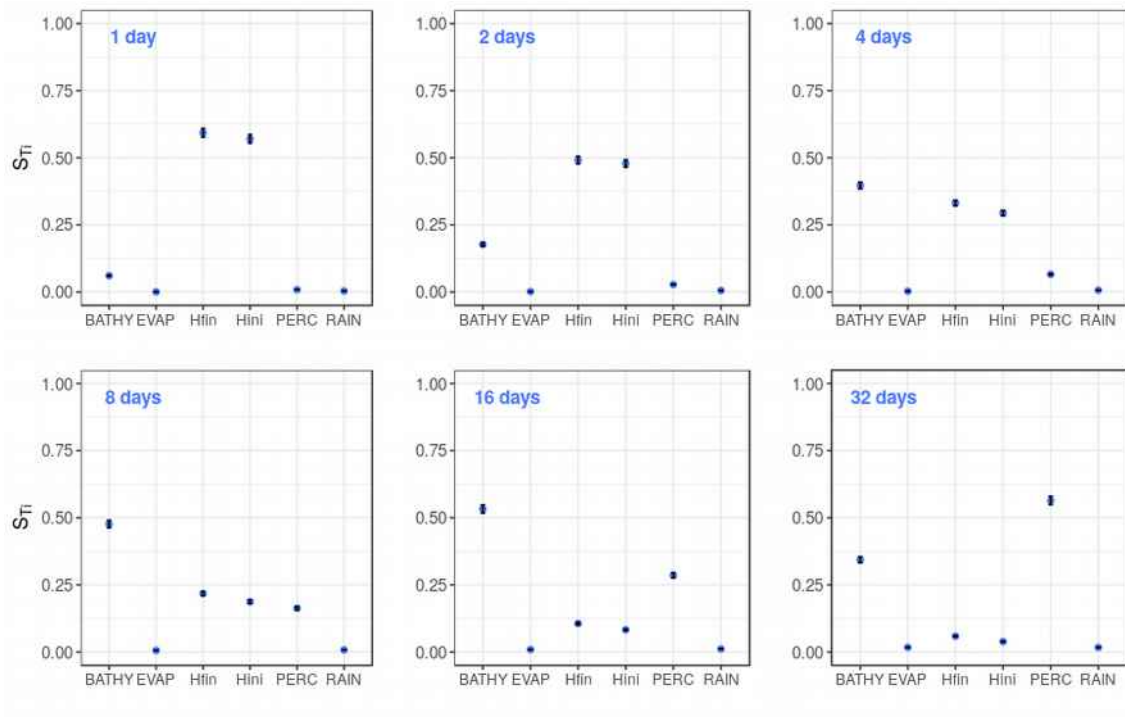
288 The stream runoff was also estimated using the coefficient runoff method. The best performance in the estimation was  
 289 obtained with a runoff coefficient of 0.09. Based on this value, the NSE ranged from 0.27 (found at 1 day temporal resolution)  
 290 to 0.54 (found at 24 days). The variation in the  $NSE_{\text{sqrt}}$  with the temporal resolution followed the same pattern as that  
 291 observed using the small reservoir method. However, the values obtained using the coefficient runoff method were lower  
 292 than those obtained using of the small reservoir method, ranging from 0.06 at the 1 day temporal resolution to 0.5-0.7 at

293 temporal resolutions greater than 9 days. The discrepancy between observations and simulations with the runoff coefficient  
294 method was found for the full range of values at all time steps (Figure 4). Unlike the reservoir method, the runoff coefficient  
295 method tended to overestimate the medium flow values ranging from  $5.0 \cdot 10^{-5}$  to  $5.0 \cdot 10^{-4}$  m/day. The reservoir method  
296 simulated also better than the coefficient runoff method the highest values larger than  $5.0 \cdot 10^{-4}$  m/day.

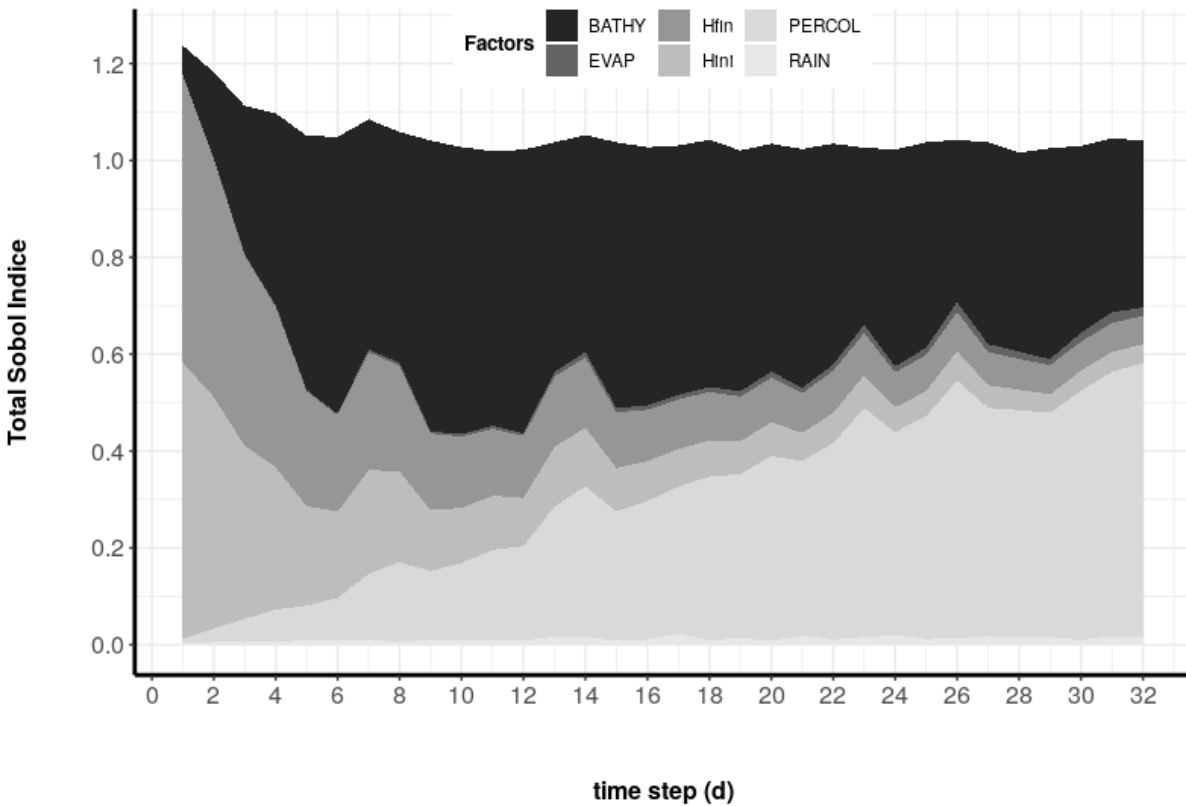
297

### 298 **3.2 Global sensitivity analysis**

299 Regarding the lowest time resolution, the  $S_T$  of the initial and final volumes are especially large with values exceeding 0.55  
300 (Figure5). The other factors, namely, bathymetric relations, evaporation, rainfall and percolation rates, have very low to  
301 almost null  $S_{Ti}$ . Regarding the highest time resolution, as illustrated by the plot at the temporal resolution of 32 days in Figure  
302 5, the percolation rate is the dominant factor in the estimation with  $S_{Ti}$  greater than 0.50. The bathymetric relation is a factor  
303 with a large  $S_{Ti}$  ( $>0.3$ ) for temporal resolution greater than 2 days. This is even the dominant factor for resolutions between 4  
304 and 23 days. The evaporation and rainfall rates have very low  $S_{Ti}$ , lower than 0.02, for all resolutions. The variation shows a  
305 progressive decrease in the  $S_{Ti}$  for the initial and final water levels as the temporal resolution increases (Figure 6). This  
306 decrease is particularly sharp up to a temporal resolution of 10 days, and then, the decreasing trend is slow. Regarding the  
307 percolation, the increase in  $S_{Ti}$  is sharp up to 10 days, after which the rate of increase is slow. Notably, the cumulative  $S_{Ti}$  of  
308 each of the six factors is lower than 1.1 at the temporal resolutions greater than 2 days. Thus, the interactions between the  
309 factors are particularly weak at these temporal resolutions.



310 Figure 5 :  $S_{T_i}$  at six time steps from (a) 1 to (f) 32 days. The  $S_{T_i}$  of the following estimated factors are provided: bathymetric  
 311 relations (BATHY), evaporation (EVAP), final and initial reservoir water levels (Hini and Hfin), percolation (PERCOL) and  
 312 direct rainfall (RAIN).



313 Figure 6 :  $S_{T_i}$  at continuous time steps from 1 to 32 days. The  $S_{T_i}$  of the following estimated factors are provided: bathymetric  
 314 relations (BATHY), evaporation (EVAP), final and initial reservoir water levels (Hini and Hfin), percolation (PERCOL) and  
 315 direct rainfall (RAIN).

#### 316 **4. Discussion**

317 The relevance of using small reservoirs as stream gauges is analysed in this study. The analysis is developed based on a  
 318 specific case study of the Kamech small reservoir, which drains a 2.64 km<sup>2</sup> catchment in northern Tunisia. Nevertheless,  
 319 general rather than only site-specific outputs can be drawn and emphasized based on the results.

##### 320 **4.1 Using small reservoirs to gauge stream runoff**

321 Using small reservoirs as stream gauges leads to globally reliable estimations of stream runoff at each time step, as  
322 illustrated by the estimation performance. However, the reliability must be nuanced according to the temporal resolution and  
323 stream runoff range. The reliability increases as the temporal resolution increases, as reflected by the variations in the mean  
324 errors and Nash efficiencies with the resolution. Furthermore, regarding the lowest temporal resolutions [1-8 days], the  
325 highest stream runoff values are estimated better than the lowest values, as indicated by the low  $NSE_{\text{sqrt}}$  (Figure 3) and the  
326 differences between the observed and estimated stream runoff values lower than  $5 \times 10^{-4}$  m/day (Figure 4). Two explanations  
327 can be offered for this phenomenon. The first explanation is provided by the uncertainty analysis. Indeed, we showed that  
328 the relative estimation uncertainty due to the uncertainties in the mass balance terms (Equation 2) is higher in low stream  
329 runoff than high stream runoff (e.g., up to 116% at a 1-day temporal resolution). The second reason is that the observed  
330 stream runoff is also affected by errors. In the Kamech catchment, the stream runoff is derived from water level  
331 measurements performed in a channel at the outlet gauge station (Figure 1). Low water levels (a few millimetres in the  
332 Kamech gauge station) may be affected by errors. Furthermore, water level measurements are performed with a pressure  
333 sensor whose error is absolute and not relative; consequently, the error in the water level measurement is higher at low  
334 water levels than high water levels.

335 As stream runoff is estimated more reliably in large stream runoff than small stream runoff, using small reservoirs as stream  
336 gauges appears particularly relevant in arid and semi-arid environments. In environments such as the Mediterranean, excess  
337 infiltration overland flow (Hortonian flow) is recognized as the main mechanism responsible for stream runoff (Ribolzi *et al.*,  
338 2000, 2007 ; Ludwig *et al.*, 1999).

339 The stream runoff in these environments is very intermittent. Furthermore, storm flow usually constitutes the predominant  
340 fraction of stream runoff, while the baseflow fraction is small and even null in some areas. In the Kamech catchment, the  
341 baseflow was estimated to account for 11% to 28% of the total stream runoff depending on the year (Raclot *et al.*, 2010).  
342 Accordingly, our results show that the implementation of small reservoir water monitoring as a stream gauging network could  
343 be particularly suitable for this type of hydrological function encountered in arid and semi-arid environments, such as the

344 Mediterranean, where the volume of stream runoff is mainly due to large storm events. In contrast, estimating stream runoff  
345 based on small reservoir monitoring during low flow periods is associated with relatively large uncertainties and errors and  
346 appears much less appropriate. In the Kamech catchment, this situation is clearly illustrated by the low values of  $NSE_{\text{sqrt}}$  at  
347 the shortest temporal resolutions (<8 days) (Figure 3). Interestingly, the stream runoff was better estimated with the small  
348 reservoir method compared to a simpler method, namely, the runoff coefficient. The runoff coefficient method, which is a  
349 simple method used to estimate stream runoff, appears to be particularly appropriate for arid and semi-arid catchments  
350 where Hortonian runoff is often the dominant process as in Kamech catchment (Hingray et al., 2014). Therefore, the  
351 difference in the performance criteria values between the two methods shows the added value that could be provided by the  
352 small-reservoir method.

353 Automatic devices, such as those employed in the Kamech catchment, are valid methods for obtaining water level  
354 measurements to estimate stream runoff. However, in remote areas, the financial cost of such devices and the maintenance  
355 needs and long-term reliability of the equipment are real concerns. Crowdsourcing has been developing in recent years in  
356 hydrology to produce new data through the involvement of citizens (Lowry et al., 2019 ; Strobl et al., 2020). As a part of the  
357 development of crowdsourcing in hydrology, collaborative and community-based approaches could be an efficient way to  
358 obtain reliable measurements while strengthening the relationships with the local populace. In the Kamech catchment, for  
359 instance, along with automatic measurements, a villager performs daily manual measurements of pan evaporation, rainfall  
360 and water levels in the reservoir.

#### 361 **4.2. Uncertainty in the stream runoff estimation**

362 The conditions that must be met to obtain reliable stream runoff estimations differ depending on the temporal resolution. At  
363 short temporal resolutions, the main uncertainty in stream runoff estimations is caused by uncertainty in the water level  
364 measurements. Decreasing the uncertainty in the estimated stream runoff could imply decreasing uncertainty in reservoir  
365 water level measurements. In the present study, the water level measurement error was fixed at 20 mm to incorporate  
366 equipment errors (the error due to the pressure sensor as given by the manufacturer) and errors arising from environmental  
367 conditions (mainly due to small wind-generated water waves). Reducing the error due to in situ sensors may be  
368 accomplished in the future by improving the measurement technology. Moreover, the errors due to wind-induced waves



369 could be reduced by performing high-frequency measurements (once every minute or less) to provide an estimate of the  
370 magnitude and filtering high-frequency variations in water level measurements. Such filtering could be achieved by applying  
371 a moving average with a window of a few minutes.

372 At large temporal resolutions (longer than 23 days in the present case), the percolation estimation is the main source of  
373 uncertainty. In many small reservoir water balance approaches, percolation is often neglected, mainly because it is difficult to  
374 estimate (Oblinger *et al.*, 2010). Nevertheless, we show that percolation estimations appear crucial for using small reservoirs  
375 as stream gauges at decadal or longer temporal resolutions. Regarding the percolation issue, the Kamech catchment is likely  
376 representative of many small reservoirs in arid and semi-arid regions. In dams built to enhance groundwater recharge, the  
377 percolation rate indeed represents a major flux in the reservoir water dynamics, as this enhancement is the aim of the  
378 reservoir. In contrast, the engineering of other reservoirs does not prevent unwanted percolation due to leaking dam walls or  
379 permeable reservoir beds. To resolve this issue, pragmatic approaches have been proposed and applied in previous studies  
380 to estimate the percolation under small reservoirs (Oblinger *et al.*, 2010 ; Fowe *et al.*, 2015). The most straightforward  
381 method is to quantify percolation from the reservoir water balance on many non-rainy days and non-flowing days, *i.e.*, days  
382 when the runoff entering the reservoir is null or negligible, and by considering the evaporation (Sharda *et al.*, 2006). Under  
383 such conditions, the percolation volume can be estimated as the reservoir volume decrease minus the evaporation volume.  
384 A relation with these estimations and corresponding water levels can often be developed and employed to estimate the  
385 percolation rate as a function of the reservoir water level.

386 Bathymetric relations (L-A and L-V) constitute a strong factor of uncertainty at all temporal resolutions and may even serve  
387 as the dominant factor at temporal resolutions ranging from 4 to 23 days. Bathymetric relations are involved in the estimation  
388 of nearly all terms in Equation 2 used for the runoff estimation. Evaporation, rainfall, and percolation volumes are area-  
389 dependent, and thus dependent on the L-A relations ; the estimation of the initial and final volumes is directly related to the L-  
390 V relations. In this study, the relations were established based on an in situ topographic survey of the reservoir bed.  
391 Performing a topographic survey for several reservoirs would not be trivial and would be a major constraint in deploying the

392 methods to many reservoirs in a region. However, the different avenues currently explored could at term overcome this  
393 constraint and provide information necessary for the estimation of the bathymetric relations. The use of a geomorphic  
394 predictor, such as that used by Sobek et al. (2014), to estimate lake water capacity and depth could be such an avenue.  
395 Developments in methodological procedures based on remote sensing and image analysis techniques at fine spatial  
396 resolutions represent another avenue. Satellite image analyses have been used to detect and estimate the water storage  
397 and surface area of small water bodies, such as reservoirs (Miahle et al. 2008; Eilander et al., 2014; Ogilvie et al., 2019). The  
398 analysis of digital elevation models could be another avenue in a context of the increasing availability of fine spatial  
399 resolution DEM. As conducted by Alcantara et al. (2010) at a large reservoir, integrating historical and Shuttle Radar  
400 Topography Mission (SRTM) topographic data prior to the reservoir construction could allow the establishment of  
401 bathymetric relations in small recent reservoirs.

402 Many studies investigating the hydrology and water balance of small reservoirs have focused on and emphasized the  
403 importance of direct evaporation from the reservoir water surface and the need to obtain reliable estimates of such flux. As  
404 evaporation is a form of water loss, knowing and preventing evaporation are indeed major concerns in the water  
405 management of small reservoirs. However, with the objective of estimating stream runoff, estimating evaporation is less  
406 crucial because it is far from a major source of uncertainty. Hence, the weight assigned to the percolation rate in the water  
407 dynamics and water balance of the Kamech reservoir in relation with water levels or bathymetric relations can justify the  
408 small sensitivity of the stream runoff estimation to the evaporation estimation uncertainty.

409

## 410 **Conclusion**

411 We analysed the relevance of using small reservoirs to gauge stream runoff. The estimations of high stream runoff are more  
412 reliable than those of low stream runoff and the performance of estimation improves as the temporal resolution increases

413 from 1 to 32 days. Using a small reservoir to gauge stream runoff appears appropriate for arid and semi-arid environments,  
414 in which stream runoff mainly comprises high magnitudes of infrequent storm runoff due to excess infiltration runoff. In  
415 addition, the uncertainty factors change depending on the temporal resolution. The main source of uncertainty is the  
416 reservoir water level at the shortest temporal resolutions, while at the longest temporal resolutions, the uncertainty in the  
417 percolation rate is the major source of uncertainty in the stream runoff estimation. The L-A and L-V relations constitute a  
418 major factor of uncertainty at temporal resolutions greater than 1 day. Therefore, using reservoirs to gauge stream runoff  
419 requires determining these relations, which currently appears to be a strong constraint in the perspective of deploying this  
420 method over a large area with a large number of reservoirs. Recent and on-going developments in procedures based on  
421 remote sensing and image analysis techniques could help eliminate this constraint. An obvious limitation of this study is that it  
422 is based on only one catchment. The same analysis could be conducted in other catchments with a wealth of data  
423 comparable to that of the Kamech catchment. At least, using small reservoirs to gauge stream runoff requires water level,  
424 rain and evaporation measurements. Acquiring such measurements can be a real challenge, especially in remote areas, due  
425 to financial costs and the maintenance and long-term reliability of monitoring infrastructures. Crowdsourcing by local villagers  
426 of these hydrological data could be a way to address this challenge and to involve the public in water resource evaluations.

## 427 **Acknowledgments**

428 The Kamech catchment belongs to the OMERE observatory ([www.obs-omere.org](http://www.obs-omere.org)), which is funded by the French  
429 organizations INRAE and IRD and coordinated by INAT (Tunis, Tunisia), INRGREF (Tunis, Tunisia), UMR Hydrosciences  
430 (Montpellier, France) and UMR LISAH (Montpellier, France). The OMERE observatory belongs to OZCAR-RI, which is  
431 supported by the French Ministry of Education and Research through the Allenvi Alliance. We thank Radhouane Hamdi  
432 (IRD), Zakia Jenhaoui (IRD) and Kilani Ben Hazez (IRD) for their tireless and rigorous efforts in maintaining the Kamech  
433 catchment observatory and collecting and processing the data. Jean-Stéphane Bailly (AgroParisTech) is also thanked for his  
434 insights into the global sensitivity analysis. We are very grateful for the constructive comments and recommendations by the  
435 three reviewers, which substantially increased the scientific quality of the manuscript.

436 **References**

- 437 J. Albergel, N. Rejeb, 1997, Les lacs collinaires en tunisie : enjeux, contraintes et perspectives. Comptes-Rendus de l'Académie  
438 d'Agriculture de France, 83(2):101–104.
- 439 E. Alcântara, E. Novo, J. Stech, A. Assireu, R. Nascimento, J. Lorenzetti, A. Souza, 2010, Integrating historical topographic maps and  
440 SRTM data to derive the bathymetry of a tropical reservoir, Journal of Hydrology, 389 (3–4), 311-316,  
441 <https://doi.org/10.1016/j.jhydrol.2010.06.008>.
- 442 M. Bouteffeha, Cécile C. Dages, R. Bouhlila, J. Molenat, 2015, A water balance approach for quantifying subsurface exchange fluxes and  
443 associated errors in hill reservoirs in semiarid regions. Hydrological processes, 29(7):1861–1872.
- 444 D. Eilander, F.O. Annor, L. Iannini, N. Van de Giesen, 2014, Remotely Sensed Monitoring of Small Reservoir Dynamics: A Bayesian  
445 Approach. *Remote Sensing*. 6(2):1191-1210. <https://doi.org/10.3390/rs6021191>
- 446 T. Fowe, H. Karambiri, J.-E. Paturel, J.-C. Poussin, P. Cecchi, 2015, Water balance of small reservoirs in the volta basin: A case study of  
447 boura reservoir in burkina faso. Agricultural Water Management, 152:99 – 109. doi: <https://doi.org/10.1016/j.agwat.2015.01.006>.
- 448 G. Fu, C. Liu, S. Chen, S., J. Hong, 2004, Investigating the conversion coefficients for free water surface evaporation of different  
449 evaporation pans. Hydrological Processes, 18: 2247-2262. <https://doi.org/10.1002/hyp.5526>
- 450 J. Gaillardet, I. Braud, F. Hankard, S. Anquetin, O. Bour, N. Dörfli, J.R. de Dreuzy, S. Galle, , other, 2018, OZCAR: The French  
451 Network of Critical Zone Observatories. Vadose Zone Journal, 33(17), doi: 10.2136/vzj2018.04.0067.
- 452 F. Habets, J. Molénat, N. Carluier, O. Douez, D. Leenhardt, 2018, The cumulative impacts of small reservoirs on hydrology: A review.  
453 Science of The Total Environment, 643:850. doi: [doi.org/10.1016/j.scitotenv.2018.06.188](https://doi.org/10.1016/j.scitotenv.2018.06.188).
- 454 E. Habib, W.F. Krajewski, A. Kruger, 2001, Sampling errors of tipping-bucket rain gauge measurements. Journal of Hydrologic

455 Engineering, 6(2):159–166.

456 B. Hingray, C. Picouet, A. Musy, 2014, Hydrology a science for engineers, CRC Press, 572p

457 I. Horner, B. Renard, J. Le Coz, F. Branger, H.K. McMillan, G. Pierrefeu, G., 2018, Impact of stage measurement errors on streamflow  
458 uncertainty. *Water Resources Research*, 54, 1952– 1976. <https://doi.org/10.1002/2017WR022039>

459 D.A. Hughes, S.K. Mantel, 2010, Estimating the uncertainty in simulating the impacts of small farm dams on streamflow regimes in south  
460 africa. *Hydrological Sciences Journal-Journal Des Sciences Hydrologiques*, 55(4):578–592. doi: 10.1080/02626667.2010.484903.

461 C. Li, Q. Wang, W. Shi, S. Zhao, 2018, Uncertainty modelling and analysis of volume calculations based on a regular grid digital elevation  
462 model (DEM), *Computers & Geosciences*, 114,117-129, <https://doi.org/10.1016/j.cageo.2018.01.002>

463 J.R. Liebe, N. van de Giesen, M. Andreini, M.T. Walter, T.S. Steenhuis, 2009, Determining watershed response in data poor  
464 environments with remotely sensed small reservoirs as runoff gauges. *Water Resources Research*, 45(7):W07410–W07410. doi:  
465 10.1029/2008wr007369.

466 C.S. Lowry CS, M.N. Fienen, D.M Halland K.F. Stepenuck, 2019, Growing Pains of Crowdsourced Stream Stage Monitoring Using  
467 Mobile Phones: The Development of CrowdHydrology. *Front. Earth Sci.* 7:128. doi: 10.3389/feart.2019.00128

468 J.A. Ludwig, D.J.Tongway, S.G. Marsden, 1999, Stripes, strands or stipples : modelling the influence of three landscape banding patterns  
469 on ressource capture and productivity in semi-arid woodlands, Australia, *Catena*, 37(1):257-273. doi :[https://doi.org/10.1016/S0341-](https://doi.org/10.1016/S0341-8162(98)00067-8)  
470 [8162\(98\)00067-8](https://doi.org/10.1016/S0341-8162(98)00067-8).

471 V. Martínez Alvarez, M.M. González-Real, A. Baille, J.M. Molina Martínez, 2007, A novel approach for estimating the pan coefficient of  
472 irrigation water reservoirs: Application to South Eastern Spain, *Agricultural Water Management*, 92 (1–2),29-40,  
473 <https://doi.org/10.1016/j.agwat.2007.04.011>.

474 F. Mialhe, Y. Gunnell, C. Mering, 2008, Synoptic assessment of water resource variability in reservoirs by remote sensing: General  
475 approach and application to the runoff harvesting systems of south India, *Water Resour. Res.*, 44, W05411,  
476 <https://doi.org/10.1029/2007WR006065>

477 H.K. McMillan, I.K. Westerberg, T. Krueger, T., 2018, Hydrological data uncertainty and its implications. *WIREs Water*. 5:e1319.  
478 <https://doi.org/10.1002/wat2.1319>

479 I. Mekki, J. Albergel, N. Ben Mechlia, M. Voltz, 2006, Assessment of overland flow variation and blue water production in a farmed semi-  
480 arid water harvesting catchment. *Physics and Chemistry of the Earth, Parts A/B/C*, 31(17):1048-1061.

481 J. Molénat, D. Raclot, R. Zitouna, P. Andrieux, G. Coulouma, D. Feurer, O. Grunberger, J.M. Lamachère, J.S. Bailly, J.L. Belotti, et al.,  
482 2018, Omere: A long-term observatory of soil and water resources, in interaction with agricultural and land management in mediterranean  
483 hilly catchments. *Vadose Zone Journal*, 17(1).

484 R. Nathan, L. Lowe, 2012, The hydrologic impacts of farm dams. *Australian Journal of Water Resources*, 16(1):75–83.

485 J.A. Oblinger, S.M.J. Moysey, R. Ravindrinath, C. Guha, 2010, A pragmatic method for estimating seepage losses for small reservoirs  
486 with application in rural india. *Journal of Hydrology*, 385(1):230 – 237. doi: <https://doi.org/10.1016/j.jhydrol.2010.02.023>.

487 D. Raclot, J. Molenat, R. Zitouna-Chebby, J.M. Lamachere, R. Hamdi, Z. Jenhaoui, A. Debebria, M. Voltz, 2010, Dynamics of stream flow  
488 generation in a small mediterranean catchment (Kamech, Tunisia) from the storm to the water year scale. In EGU General Assembly  
489 Conference Abstracts, volume 12, page 11750.

490 Razavi, S., H. V. Gupta (2015), What do we mean by sensitivity analysis? The need for comprehensive characterization of “global”  
491 sensitivity in Earth and Environmental systems models, *Water Resour. Res.*, 51, 3070– 3092, doi:10.1002/2014WR016527

492 O Ribolzi, P Andrieux, V Valles, R Bouzigues, T Bariac, M Voltz, 2000, Contribution of groundwater and overland flows to storm flow

493 generation in a cultivated mediterranean catchment. quantification by natural chemical tracing. *Journal of Hydrology*, 233(1):241–257.

494 O. Ribolzi, H. Karambiri, T. Bariac, M. Benedetti, S. Caquineaux, M. Descloitres, A. Avenirier, 2007, Mechanisms affecting stormflow  
495 generation and solute behaviour in a Sahelian headwater catchment, *Journal of hydrology*, 337 (1-2), 104-116.

496 S.Y. Schreider, A.J. Jakeman, R. Letcher, R.J. Nathan, B.P. Neal, S.G. Beavis, 2002, Detecting changes in streamflow response to  
497 changes in non-climatic catchment conditions: farm dam development in the murraydarling basin, australia. *Journal of Hydrology*, 262(1-  
498 4): 84–98. doi: 10.1016/s0022-389 1694(02)00023-9.

499 V.N. Sharda, R.S. Kurothe, D.R. Sena, V.C. Pande, S.P. Tiwari, 2006, Estimation of groundwater recharge from water storage structures  
500 in a semi-arid climate of india. *Journal of Hydrology*, 329(1):224 – 243.

501 I.M. Sobol, 2001, Global sensitivity indices for nonlinear mathematical models and their Monte Carlo estimates, *Math. Comput. Simul.*,  
502 55, 271 – 280.

503 E. Starkey, G. Parkin, S. Birkinshaw, A. Large, P. Quinn, C. Gibson, 2017, Demonstrating the value of 400 community-based (citizen  
504 science) observations for catchment modelling and characterisation. *Journal 24401 of Hydrology*, 548:801 – 817.  
505 <https://doi.org/10.1016/j.jhydrol.2017.03.019>.

506 B. Strobl, S. Etter, I. van Meerveld, J. Seibert, 2020, Accuracy of crowdsourced streamflow and stream level class estimates.  
507 *Hydrological Sciences Journal, Special Issue: Hydrological Data: Opportunities and Barriers*, 65(5),  
508 <https://doi.org/10.1080/02626667.2019.1578966>

509 Y. Tang, P. Reed, K. van Werkhoven, T. Wagener, 2007, Advancing the identification and evaluation of 404 distributed rainfall-runoff  
510 models using global sensitivity analysis, *Water Resources Research*, 43(6). doi: 10.1029/2006WR005813.

511 J. Wang, B.L. Fisher, D.B. Wolff, 2008, Estimating rain rates from tipping-bucket rain gauge measurements. *Journal of Atmospheric and*  
512 *Oceanic Technology*, 25(1):43–56, 2008.

513 T.C. Winter, 1981, Uncertainties in estimating the water balance of lakes. JAWRA Journal of the American Water Resources Association,  
514 17: 82-115. <https://doi.org/10.1111/j.1752-1688.1981.tb02593.x>

ACCEPTED VERSION